Pure & Appl. Chem., Vol. 64, No. 7, pp. 1015–1028, 1992.
Printed in Great Britain.

INTERNATIONAL UNION OF PURE
AND APPLIED CHEMISTRY

ANALYTICAL CHEMISTRY DIVISION
COMMISSION ON ELECTROANALYTICAL CHEMISTRY*

REACTANT ADSORPTION IN ANALYTICAL PULSE VOLTAMMETRY: METHODOLOGY AND RECOMMENDATIONS

(Technical Report)

Prepared for publication by

HERMAN P. VAN LEEUWEN[1], JACQUES BUFFLE[2] and MILIVOJ LOVRIĆ[3]

[1]Wageningen Agricultural University, Dreijenplein 6, 6703 HB Wageningen, Netherlands
[2]University of Geneva, Sciences-II, 30 Quai E. Ansermet, 1211 Geneva 4, Switzerland
[3]Centre for Marine Research, Rudjer Boskovic Institute, POB 1014, Zagreb 41001, Croatia

*Membership of the Commission during the period (1987–91) when this report was prepared was as follows:

Chairman: 1987–89 M. Senda (Japan); 1989–91 R. A. Durst (USA); *Vice Chairman*: 1987–89 R. Kalvoda (Czechoslovakia); 1989–91 M. Senda (Japan); *Secretary*: 1987–89 R. A. Durst (USA); 1989–91 K. M. Kadish (USA); *Titular Members*: R. P. Buck (1989–91; USA); J. Buffle (1987–89; Switzerland); M. Gross (1987–91; France); K. M. Kadish (1987–89; USA); K. Štulik (1989–91; Czechoslovakia); K. Tóth (1987–91; Hungary); *Associate Members*: A. M. Bond (1989–91; Australia); R. P. Buck (1987–89; USA); K. Cammann (1989–91; FRG); M. Filomena Camoes (1987–91; Portugal); W. Davison (1987–89; UK); A. Fogg (1987–91; UK); H. Kao (1987–89; China); R. C. Kapoor (1987–89; India); W. Kutner (1989–91; Poland); T. Kuwana (1989–91; USA); M. L'Her (1989–91; France); J. G. Osteryoung (1987–89; USA); G. Prabhakara Rao (1989–91; India); S. Rondinini Cavallari (1987–91; Italy); K. Štulik (1987–89; Czechoslovakia); Y. Umezawa (1987–91; Japan); H. P. van Leeuwen (1987–91; Netherlands); E. Wang (1987–91; China); *National Representatives*: G. E. Batley (1987–91; Australia); B. Gilbert (1987–89; Belgium); H.-Y. Chen (1990–91; Chinese Chemical Society); A. A. Vlček (1987–91; Czechoslovakia); H. B. Nielsen (1987–89; Denmark); H. B. Kristensen (1988–91; Denmark); K. Cammann (1987–89; FRG); M. L'Her (1987–89; France); E. Lindner (1987–91; Hungary); G. Prabhakara Rao (1987–89; India); R. C. Kapoor (1989–91; India); W. F. Smyth (1987–91; Ireland); E. Grushka (1987–91; Israel); T. Mussini (1989–91; Italy); K. Izutsu (1987–91; Japan); A. J. McQuillan (1987–91; NZ); Z. Galus (1987–91; Poland); J. Galvez (1987–91; Spain); G. Johansson (1987–91; Sweden); G. Somer (1987–91; Turkey); A. K. Covington (1987–91; UK); J. F. Coetzee (1987–89; USA); W. F. Koch (1989–91; USA); I. Piljak (1987–91; Yugoslavia).

Reactant adsorption in analytical pulse voltammetry: Methodology and recommendations (Technical Report)

ABSTRACT

This report surveys the effects that arise in pulse voltammetric analysis if the reactant is adsorbed at the *electrode/solution interface*. Modifications of normal and differential pulse polarograms are outlined. Suitable methodology is developed on the basis of available theory and experimental evidence. The report is concluded with guide-lines for detecting reactant adsorption as well as recommendations for properly dealing with them in practical analytical situations.

1. INTRODUCTION

Pulse voltammetry/polarography has developed into a widespread analytical method, with numerous applications in all kinds of practical areas such as pharmaceutical, clinical and environmental chemistry (see for example refs. 1-3). With the growth of the number of applications, including those to a great many organic compounds, the phenomenon of reactant adsorption has gained importance. Adsorption of the electroactive analyte onto the mercury electrode may be the result of surface activity of the reacting species themselves, or due to a surface active electroinactive component in the sample which induces adsorption of the reactant. A well-known example in the latter category is the induced adsorption of metal ions in systems with adsorbing ligands. Systems for which reactant adsorption has definitely been shown to affect the pulse polarogram are for instance Cu^{I}, Cu^{II}, Cd^{II}, Zn^{II}, Pb^{II} in solutions containing bromide [4], iodide [5], pyrocatechol [6,7], amino acids [8], fulvic/humic acids [9] benzene/pyridine carboxylic acids [10], polyelectrolytes [11] and solutions of nitro compounds [12], pyridines, substituted pyridine *N*-oxides, substituted azobenzenes [13], DNA [14], chloramphenicol [15], berberine [16]. *This list is certainly not exhaustive and keeps on growing.*

The outer signs of reactant adsorption are most evident with normal pulse polarography (NPP). For not too weak adsorption the wave shows a maximum with a magnitude that increases with decreasing pulse duration. Beyond the maximum, the wave reaches a limiting current which (i) is depressed as compared to the adsorption-free case, and (ii) depends on pulse duration in a typical manner. In differential pulse polarography (DPP), reactant adsorption may lead to peak enhancement or - for strong adsorption - to serious deformation or splitting of the peak. Again the dependence of the peak current on the timing characteristics (pulse duration and drop period) shows deviations from diffusion-controlled behaviour. An important difference between NPP and DPP is that adsorption takes place at the freely selectable initial potential in the former case and successive potentials along the ramp in the latter.

In the practical utilization of pulse polarography it is essential that the analyst may deal - in some way or another - with the effects of adsorption. Depending on the particular situation there are several options. First it is possible to use the results of the many theoretical studies recently made. Explicit expressions for the analytical parameters are available for a number of situations. Alternatively, numerically simulated polarograms may be fitted to experimental data in order to find an unknown analyte concentration (together with the adsorption parameters). On a more pragmatic level the effects of reactant adsorption are sometimes

- taken as they are, together with the correspondingly distorted calibration curves, or
- enhanced, thus increasing the sensitivity for the particular case, or
- eliminated.

The aim of this report is to

(i) summarize and explain the phenomena arising from reactant adsorption in pulse polarography,

(ii) survey the theoretical achievements, especially in as far as they are of relevance to analytical pulse polarography, and

(iii) outline the methodological guide-lines for dealing with the effects of reactant adsorption in practical pulse polarographic analysis.

Due to the recent intensive theoretical attention for reactant adsorption in pulse voltammetry, the subject is better developed on the theoretical level then on the experimental one. In connection with that, this report will concentrate on the methodological features as derived from theory, rather than scrutinize the available better experimental evidence.

2. SURVEY OF PHENOMENA DUE TO REACTANT ADSORPTION

A qualitative outline of the effects of reactant adsorption in a pulse polarographic experiment is most easily given in terms of a normal pulse polarogram. The NPP waveform and the symbols used are given in Fig. 1. The NPP case is basically simpler since in the delay period before pulse application there is no faradaic reaction coupled to the adsorption process. Let us consider a surface active reactant O that can be reduced to product R

$$\begin{array}{l} O_s + ne \rightleftarrows R_s \\ \uparrow\downarrow \\ O_a \end{array} \qquad (1)$$

where the subscripts s and a refer to solution and adsorbed state, respectively.

Below we shall consider the interfacial adsorption/desorption process infinitely fast and we shall ignore the differentiation between the reduction of O in solution (O_s) and O in the adsorbed state (O_a). Typically for the NPP case, the initial potential E_i is much more positive than $E_{1/2}$. At $E = E_i$, a certain surface excess Γ_O is built up during the period from $t = 0$ to $t = t_0$. Generally, the magnitude of Γ_O at $t = t_0$ is not the equilibrium value (as related to the bulk concentration c_O^*) and c_O just outside the adsorbed layer is still lower than c_O^*. This general situation at $t = t_0$ is sketched in Fig. 2. The adsorptive depletion layer has a thickness δ_0, which depends on the diffusion coefficient D_O and t_0. Depending on the nature of the adsorption isotherm, the exact course of the concentration profile at $t = t_0$ may be quite complicated. The actual concentration at the surface gradually increases with time and the gradient $(dc_O/dx)_{x=0}$ decreases with time. Limiting cases are for

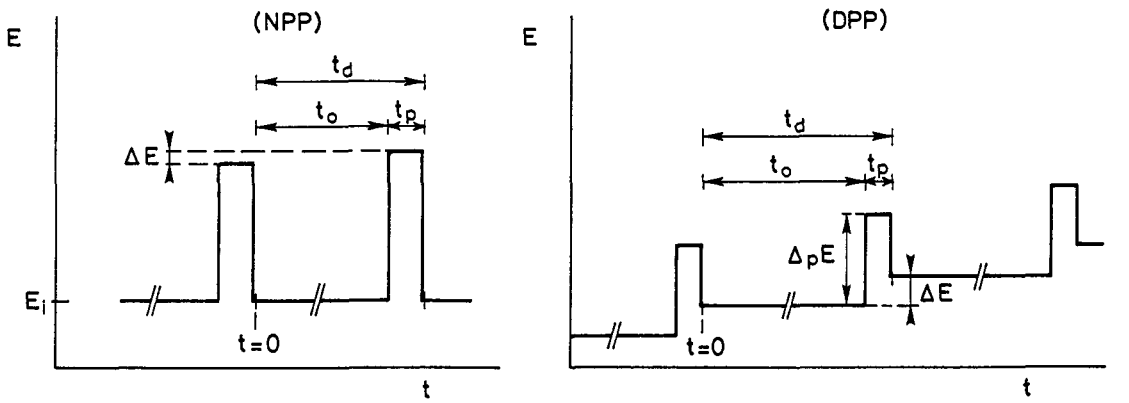

Fig. 1 Definition of the NPP and DPP waveforms and the timing parameters.

example $c_O(x=0) = 0$ together with $(dc_O/dx)_{x=0} = c_O^*/\delta_0$ - for infinitely strong adsorption outside the saturation regime -, or $\Gamma_O = \Gamma_O^{max}$ together with $(dc_O/dx)_{x=0} = 0$ for the case of reaching full coverage before $t = t_0$. Apparently, these cases correspond to limits for low and high reactant concentrations, respectively.

Under conditions of not too strong adsorption, the pulse polarographic response at potentials near or somewhat negative from $E_{1/2}$ is governed by both diffusion of O and reduction of adsorbed O. It is perhaps helpful to consider that the faradaic current in that potential region is composed of two elements which have different time dependencies. The diffusion - controlled flux $D_O(dc_O/dx)_{x=0}$ basically follows some $t^{-1/2}$ dependence (albeit a distorted one due to the foregoing adsorption process). The contribution from reduction of adsorbed O, $d\Gamma_O/dt$, does not involve any transport towards the electrode surface and follows a more progressive decrease with time (pseudo-capacitive behavior). Especially for low t_p, the current due to reduction of adsorbed reactant may be much larger than the diffusion current and correspondingly high total currents may result. Fig. 3 illustrates this. With increasingly negative potential, $c_O(x=0)$ decreases and so does Γ_O. In the supposedly Nernstian case the magnitude of $d\Gamma_O/dt$, as well as the corresponding current component, is mainly limited by diffusion of R. Thus with decreasing E, curve 2 of Fig. 3 gets a larger amplitude and a smaller time constant. The corresponding current component gradually disappears from the experimental sampling time window and only the diffusional component remains. As usual, this latter current component becomes maximal in the limit for $c_O(x=0)=0$. The usual NPP conditions imply that $t_p << t_0$ so that the pulse diffusion layer thickness δ_p is much smaller than δ_0. The consequence is that the limiting diffusion current is lower than in the adsorption-free situation. With reference to Fig. 2 one might say that the pulse electrolysis only covers a small part of the adsorptive depletion layer and thus "sees" an apparent concentration c_O, smaller than c_O^*. This is the basic reason for the observed depression of the NPP limiting current.

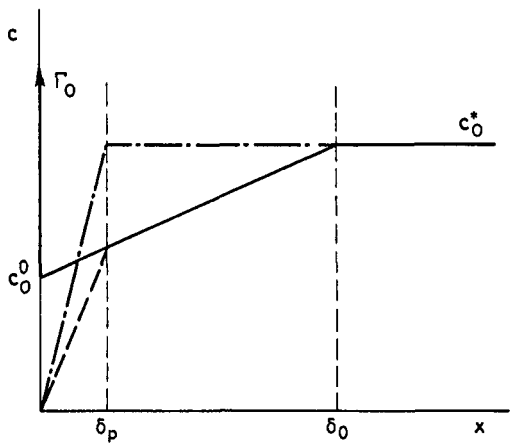

Fig. 2. Schematized concentration profile (i) at $t = t_0$, after adsorption of the reactant O at $E = E_i$ during the delay period from $t = 0$ to $t = t_0$ (——); (ii) at $t = t_0+t_p$ in the limiting current region (---); (iii) as (ii) but for the case of no adsorption (·····).

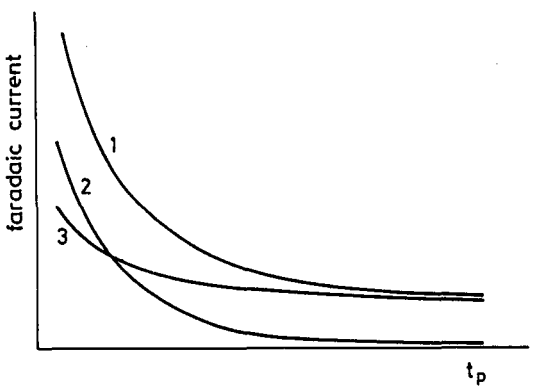

Fig. 3. NPP current, time dependence in case of reactant adsorption. 1: observed total current; 2 : current due to reduction of adsorbed reactant; 3 : diffusional current

The qualitative reasoning above leads to an NPP polarogram with a shape as sketched in Fig. 4a. At the onset of the wave, the contributions from reduction of adsorbed reactant give rise to a maximum. Eventually a limiting current is obtained, but this is depressed as compared to the adsorption-free case. For stronger adsorption, the reduction of adsorbed reactant is shifted towards more negative potentials, resulting in a maximum superimposed on the limiting current (a "post-peak"). Though not extensively discussed here, we

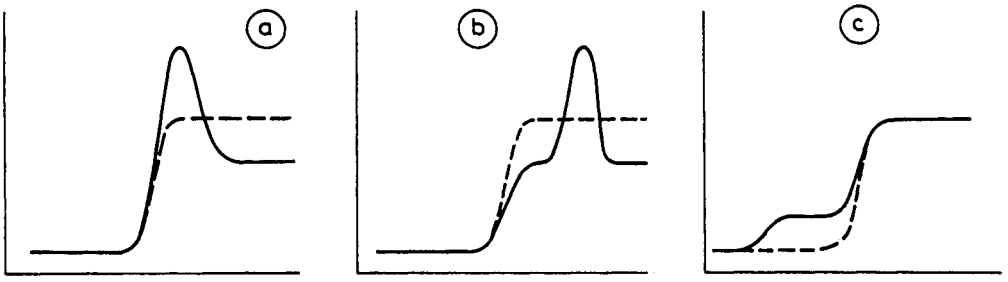

Fig. 4. Modification of the NP polarogram due to adsorption. a) weak to intermediate reactant adsorption; b) strong reactant adsorption, yielding a "post-peak"; c) strong adsorption of product, yielding a "pre-wave". The interrupted curve is the reference case of no adsorption.

add for comparison the NPP polarogram for the case of strong adsorption of the reduction product R. For sufficiently high reactant concentrations, one would see a so-called "pre-wave" which is related to the formation of a layer of adsorbed R.

The already sufficiently complicated picture may still change with reactant concentration. For strong adsorption and low concentration, the NPP limiting current approaches the d.c. value. Wave 4b then loses its initial part and has the shape of curve 4a; its shift along the potential axis is directly related to the adsorption strength. Polarogram 4c loses its "main" wave for concentrations below the value necessary to warrant full coverage before pulse application. The position of the wave is determined by the ratio between the adsorption affinities of the oxidized and reduced species (this ratio being $<< 1$).

For differential pulse polarography (DPP) the reasoning is more intricate. Adsorption takes place at potentials which move through the range selected. In the pre-pulse period the adsorption and the faradaic reaction can proceed simultaneously. Moreover, the potential dependence of the adsorption may play a significant role. Nevertheless, the basic ideas that led us to the concentration profile in Fig. 2 may still be helpful, albeit on an even more qualitative level. Partial reduction of adsorbed reactant enhances the DPP current too. For not too strong adsorption and especially for small t_p values, this may result in an increase of the DPP peak height (Fig. 5a). Peak enhancement in DPP is the analogue of the maximum at the onset of the wave in NPP (compare Fig. 4a). As in NPP, the reduction of adsorbed reactant is shifted toward negative potentials with increasing strength of adsorption. Consequently, a separate peak may be observed at $E < E_{1/2}$ for strong reactant adsorption (Fig. 5b) or at $E > E_{1/2}$ for strong product adsorption (Fig. 5c). As before the current component due to conversion of adsorbed material depends strongly on t_p, the time dependence is much stronger than for the diffusion-controlled current. For detection of adsorption this feature may be more important than the shape of the DPP polarogram, which only in rather extreme cases shows the distortions as in Figs. 5b and 5c. It is to be noted again that the shapes of Figs. 5b and 5c change with changing reactant concentration, in a way analogous to what was said about Figs. 4b and 4c.

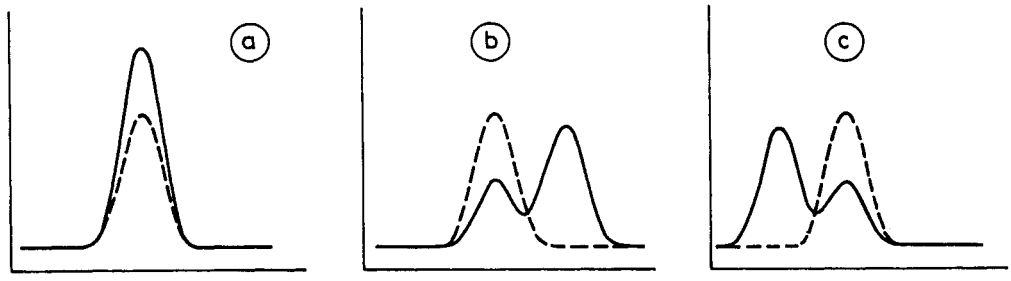

Fig. 5. Modification of the DPP polarogram due to adsorption. a) weak to intermediate reactant adsorption; b) strong reactant adsorption, yielding a "post-peak"; c) strong product adsorption, yielding a "pre-peak". The interrupted curve is the reference case of no adsorption.

3. SURVEY OF QUANTITATIVE THEORY

In a form more general than eqn. (1), the scheme of the electrode process may be written as

$$\begin{array}{ccc} O_s + ne & \overset{(A)}{\rightleftarrows} & R_s \\ (B)\downarrow\uparrow & & \uparrow\downarrow(C) \\ O_a + ne & \underset{(D)}{\rightleftarrows} & R_a \end{array} \qquad (2)$$

which implies a distinction between the standard redox potential for the solution and that for the adsorbed state (that is, unless the adsorption coefficients of O and R are identical). The various steps are denoted as A to D and will be referred to as such. The starting point of the theory is formed by the continuity equations for O and R, which are applied to the continuous phase (the solution). Ignoring activity effects,

$$\frac{\partial c_i}{\partial t} = D_i \nabla^2 c_i \qquad (i = O,R) \qquad (3)$$

Provided that the adsorption/desorption reactions (steps B and C in eqn. (2)) are sufficiently fast to warrant equilibrium, the relation between c_i at the electrode surface just outside the adsorbed layer (c_i^o) and the surface excess Γ_i is given by the isotherm

$$\Gamma_i = f(c_i^o) \qquad (4)$$

In the linear Henry regime, eqn. (4) takes the simplest form

$$\Gamma_i = K_i(c_i^o) \qquad (5)$$

where K_i is the Henry coefficient for species i.

Many pulse polargraphic experiments are involved with parts of the isotherm that are well beyond the linear regime. Specification of (4) in terms of e.g. Langmuir or Frumkin isotherms is then necessary.

The current density j is directly related to the surface flux balances of the electroactive species. E.g. for semi-infinite one-dimensional diffusion the relation reads

$$x=0: \quad \frac{j}{nF} = \mp D_i \frac{\partial c_i}{\partial x} \pm \frac{d\Gamma_i}{dt} \qquad (6)$$

with for i=O the upper signs and for i=R the lower ones.

If the actual electron transfer reaction (step A or D in scheme (2)) is sufficiently fast, its rate does not affect the voltammetric signal (on the selected timescale), and we may apply the Nernst equation to the volume concentrations of O and R at the electrode surface

$$c_O^o / c_R^o = \exp\left[nF(E - E_o)/RT\right] \qquad (7)$$

or, equivalently, to Γ_O and Γ_R with the corresponding standard redox potential. If, on the other hand, irreversibility plays a role, the Nernst equation does not apply to the interfacial situation and we must envisage electron transfer rate equations of the type [17]

$$\begin{aligned} \frac{j}{nF} = & -k_A\left\{c_O^o \exp(-\alpha_A\phi_A) - c_R^o \exp[(1-\alpha_A)\phi_A]\right\} \\ & -k_D\left\{\Gamma_O \exp(-\alpha_D\phi_D) - \Gamma_R \exp[(1-\alpha_D)\phi_D]\right\} \end{aligned} \qquad (8)$$

where
- k_A and k_D are the standard rate constants for the electron transfer reactions of the dissolved and adsorbed species respectively [Note the different dimensions]
- α_A and α_D are the corresponding transfer coefficients
- ϕ_A and ϕ_D are $nF(E-E^0)/RT$ and $nF(E-E_a^0)/RT$ respectively, E_a^0 being the standard potential for the redox reaction in the adsorbed state (D).

It may be noted that most electron transfer reactions complicated by reactant/product adsorption are either reversible or totally irreversible. The majority of electrode reactions of metal ions are reversible on the pulse polarographic time-scale, whereas those of some organic molecules may be totally irreversible if the charge transfer is followed by fast and irreversible protonation of the product. Reactions of organic molecules which do not include irreversible protonation are likely to be reversible (e.g. the methylene blue/leucomethylene blue couple).

As a next step, one has to formulate the initial conditions and boundary conditions. These may differ from one experiment to another. Here we consider by way of example the case where only O is present in solution and where the electrode is not in contact with the solution before $t = 0$. We then have for the planar geometry

$$\left.\begin{aligned} t = 0,\ x \geq 0: &\begin{cases} c_O = c_O^*,\ c_R = 0 \\ \Gamma_O = \Gamma_R = 0 \end{cases} \\ t > 0,\ x \to \infty: &\ c_O = c_O^*,\ c_R = 0 \end{aligned}\right\} \qquad (9)$$

and

			NPP	DPP
$t > 0,\ x = 0$	$0 < t < t_0$	m-th cycle	$E = E_i$	$E = m\Delta E$
	$t_0 < t < (t_0 + t_p)$	m-th cycle	$E = m\Delta E$	$E = m\Delta E + \Delta_p E$
	j: eqn. (6) + eqn. (7) reversible case eqn. (6) + eqn. (8) quasi-reversible case			

(10)

where ΔE is the potential increment per cycle and $\Delta_p E$ is the pulse amplitude in DPP.
In NPP, the initial potential E_i is normally chosen well positive from E^0 so that for the pre-pulse period $c_O^0 / c_R^0 \to \infty$, $\Gamma_R \to 0$ and $j \to 0$. What remains from eqn. (6) is the flux equation for the purely adsorptive diffusional transport of O.

Equation (6) applies to the case of a stationary planar electrode. Other geometries require different expressions. For example, in case of a stationary spherical electrode such as the static mercury drop electrode, eqns. (3) and (6) take the form

$$\frac{\partial c_i}{\partial t} = D_i \frac{\partial^2 c_i}{\partial r^2} + 2\frac{D_i}{r}\frac{\partial c_i}{\partial r} \qquad (11)$$

$$r = r_0: \quad \frac{j}{nF} = \mp D_i \frac{\partial c_i}{\partial r} \pm \frac{d\Gamma_i}{dt} \qquad (12)$$

where r is the radial coordinate and r_0 the electrode radius. Expressions for other geometries may be found in the standard electrochemical literature (e.g. ref. 18).

Solutions of the above sets of equations have been presented at various levels and for a variety of conditions. Rather than explaining all results in some detail, we shall specify here the cases treated thus far. Table I collects the developments in chronological order. Main contributions are due to Barker and Bolzan (first explanation of NPP maxima in terms of reactant adsorption) Flanagan et al. (first simulations of the main effects), Van Leeuwen et al. (quantitative analytical expressions for NPP limiting current) and Lovrić (rigorous simulation of full NPP and DPP waves, including complications such as irreversibility). Work in this field has been reviewed recently by Osteryoung and Schreiner [19].

TABLE I. Survey of development of theory

NPP and/or DPP	scheme considered [as ref. to eqn. (2)]	electrode geometry	type of isotherm	further features	response considered	level of mathematical solution	remarks	references (chronological order)
N	A,B	planar	linear	reversible c.t.	full wave	semi-quantitative analytical	adsorptive depletion neglected	Barker and Bolzan[4]
D	A,B,C*	planar	linear	reversible c.t.	peak current	numerical evaluation of analytical expression	faradaic current before pulse and adsorptive depletion neglected	Anson et al. [20]
D	A,B and A,C	expanding plane	Frumkin	reversible c.t.	full peak	digital simulation	showing e.g. peak splitting due to non-linearity	Flanagan et al. [21]
N	A,B,C	expanding plane	linear, Langmuir, Frumkin	reversible c.t.	full wave	digital simulation		Flanagan et al. [5]
N D	A,B	planar		reversible c.t.	limiting/peak current	semi-quantitative analytical	linear concentration profile assumed	Van Leeuwen [22]
N	A,B	planar	linear or saturation	reversible c.t.	limiting current	analytical (series approx.)		Van Leeuwen et al. [23]
N D	A with adsorption intermediate	planar	Langmuir	both c.t.'s reversible	full wave	analytical (Henry regime) numerical (Langmuir)		Lovric [24]
N	A,B	spherical	linear or saturation	reversible c.t.	limiting current	analytical (series approx.)		Holub and van Leeuwen [25]
N	A,B(i); A,B,D(ii)	planar	Langmuir	reversible c.t.	limiting current (i); full wave (ii)	analytical solution for some limits (i); numerical simulation (ii)		Lovric [26]
N D	A with adsorption intermediate	planar	Frumkin	reversible c.t.	full wave plus capacitive current	numerical		Lovric [27]
N	A,B and $O_a \rightleftarrows R_s$	planar	linear	irreversible c.t.	full wave	analytical	includes recursive expression for Γ_O	Lovric [28]
N	A,C	planar	linear	reversible c.t. finite rates of adsorption/desorption	prewaves	numerical	adsorption-kinetic prewave	Komorsky-Lovric and Lovric [29]
N D	A,B,C	expanding plane	Langmuir	reversible c.t.	full wave/peak	semi-analytical*)	"Levich-Guidelli" and "Koryta-Laviron" approx.	Puy et al. [30]
N	A,B and $O_a \rightleftarrows R_s$	planar	linear	quasi-reversible c.t.	full wave	semi-analytical*)	includes kinetically controlled maxima	Komorsky-Lovric and Lovric [16]
N	A,B	expanding plane	linear or saturation	reversible c.t.	limiting current	analytical (series approx.)		Holub and van Leeuwen [31]
N	A,B	planar	Langmuir	reversible c.t.	limiting current	analytical (series approx.)		Van Leeuwen et al [32]
N	A,B,C,D and $O_a \rightleftarrows R_s$ $O_s \rightleftarrows R_a$	planar	linear	quasi-reversible c.t.	full wave	semi-analytical*)	incl. criteria for reversibility of O_a+ ne $\rightleftarrows$ R_a	Lovric [17]
D	A,B,C,D	planar	linear	quasi-reversible c.t.	full peak	semi-analytical*)		Lovric [33]
N	A,B,C,D	planar	linear	quasi-reversible c.t.	full wave	semi-analytical*)	adsorption of product predominant	Lovric [34]
N	A,B,C	expanding plane	Frumkin	reversible c.t.	full wave	digital simulation	using Flanagan's programs	Kobayashi [35]
N D	A,B,C	planar	linear	reversible c.t.	full wave/peak	analytical (power series)	incl. treatment RPP	Galvez et al. [36]
	*) In case of a reversible c.t., step D is implicitly included in the scheme A,B,C			c.t. = charge transfer reaction		*) involves numerical evaluation of integral equation		

4. GUIDELINES FOR ANALYTICAL PRACTICE

Since the consequences of reactant adsorption may be quite drastic, we devote a separate section to practical analytical aspects. Not only shall we point out proper ways to interpret experimental pulse polarograms affected by adsorption, we will also indicate possibilities either to eliminate or (deliberately) enhance adsorption effects, as a way to improve the quality of the analysis.

A. Dependence of currents on reactant concentration

If the adsorption conditions are constant within a series of analytical experiments - a restriction that may well be more severe than it seems -, the analytical difficulties arising from reactant adsorption are caused by non-linearity of the isotherm. As long as the adsorption is in the linear Henry regime, the NPP limiting current density j_ℓ and the DPP peak current density j_p vary linearly with c_O^* (provided the timing parameters t_0 and t_p are kept constant). This feature can be easily understood in the sense that all processes involved, i.e. accumulation of O at the electrode surface and depletion in the adsorptive diffusion layer, are linearly proportional to c_O^*. Thus we find that j_ℓ and j_p depend linearly on c_O^*, although the slopes of the j_ℓ,c^* and j_p,c^* plots differ from those of the adsorption-free case. By way of example fig. 6 shows the dependence of j_p on c^* as calculated by Flanagan et al [21] for Frumkin and Langmuir isotherms, together with experiment-al DPP data for Cd^{II} in KI/KNO_3 solutions. In the low concentration regime, roughly below 10^{-5} mol·dm^{-3} for the usual values of t_0 and $D_{reactant}$, j_p is enlarged as compared to the adsorption-free case. Due to its pseudo-capacitive nature, the enhancement increases progressively with decreasing t_p, as shown in some detail by Galvez's calculations [36].

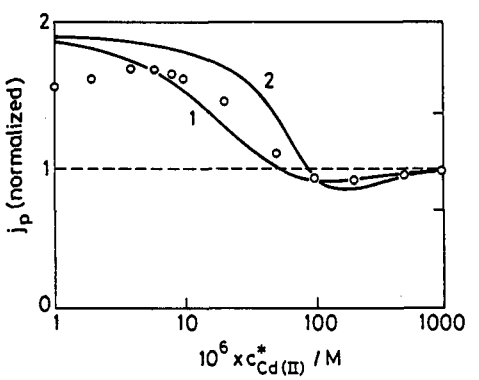

Fig. 6. Concentration dependence of DPP peak current densities (j_p), normalized with respect to the case of no adsorption. The drawn curves are obtained by digital simulation using the Frumkin (1) and Langmuir (2) isotherms. The points are experimental data for Cd(II) in 0.1 mol·dm^{-3} KI/0.9 mol·dm^{-3} KNO_3 (adapted from ref. 21).

NPP limiting currents reflect the adsorptive depletion as generated during the pre-pulse period and hence are *always smaller* than those for the adsorption-free case. As for DPP, the NPP calibration curve starts with a linear portion in the Henry regime and then bends towards higher slopes. Since j_ℓ derives from the reactant concentration profile outside the adsorbed layer, it only gradually returns to the adsorption-free calibration curve. The difference only disappears if c^* is high enough to allow for complete dismantlement of the adsorptive diffusion layer. This coincides with reaching the equilibrium value of Γ_O, unless saturation was already reached at lower c_O^*. Note that the DPP signal reflects both the accumulated reactant in the adsorbed layer and the depletion in the adsorptive diffusion layer. Therefore the DPP peak current j_p may be enhanced in one range of c^* and depressed in another (compare the intermediate range of c^* in Fig. 6). In summary, the general shapes of NPP and DPP calibration curves are shown in Fig. 7.

The situation may become more complicated if - due to strong adsorption - split peaks (DPP) or pre(post) waves (NPP) appear. The discussion above would then refer to the sum of the peak heights (DPP) or the total wave height (NPP). All components of the polarograms are in some way related to the adsorption isotherm and use of only one of the two peaks or waves does not offer special analytical advantages. The

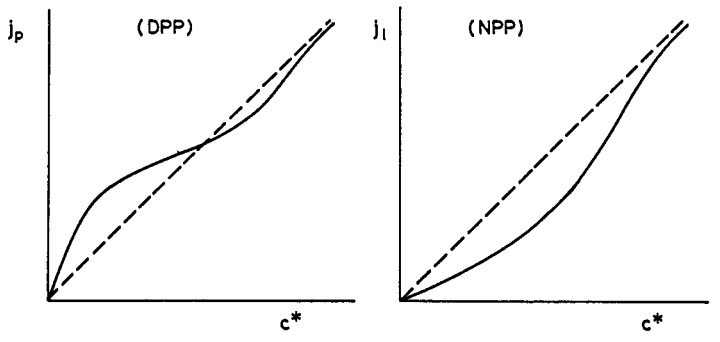

Fig. 7.
Typical shapes of analytical DPP and NPP calibration curves affected by reactant adsorption. Dashed lines correspond to no adsorption.

situation may be different if one has special intentions (such as to separate reduction form the adsorbed state and that of dissolved species). The adsorption-controlled shift of DPP peaks and NPP waves on the potential axis is of interest if one wants to measure adsorption parameters. Theoretical details may be found in the papers by Lovrić [26,34], Sanz et al. [30] and Galvez et al. [36]. A nice experimental illustration has been provided by Buffle et al. [10] in a study of adsorption of Cd^{II} and Pb^{II} complexes with fulvic-like organic ligands. By utilizing the characteristics of the NPP maximum as well as the limiting current, the nature of adsorbed metal species could be revealed.

B. Analytical utilization of elimination of reactant adsorption

Enhancement of DPP peak currents and NPP current maxima by reactant adsorption is analytically interesting since it increases the sensitivity of the pulse polarographic method. Promotion of adsorption by selecting the most favourable electrolyte and solvent can be useful, but it is probably not very practical in the analysis of many-component samples. The NPP method has the great advantage that the potential of adsorption can be chosen freely at a value where the adsorption is optimal. Combination with sufficiently short t_p values may give spectacular results at very low concentrations. For example, Van Leeuwen [37] found tremendous enlargement of the NPP maximum in the t_p range between 1 and 5 ms for aqueous solutions of methylene blue (see Fig. 8). Thus the height of the NPP maximum has potential as a sensitive analytical parameter.

Perhaps of greater practical importance are the possibilities for eliminating the effects of reactant adsorption. Apart from chemical interventions in the sample solution, there are a number of methodological possibilities to eliminate reactant adsorption effects:

(1) modification of the potential waveform

In NPP it is sometimes possible to find a value for E_i where adsorption does not occur. For systems in which the product of the electrode reaction is not adsorbed, one can simply choose E_i somewhere in the limiting current region and scan in the opposite direction. This version is denoted as reverse pulse polarography (RPP). Nice examples of this are found with the pulse polarography of heavy metals in the presence of natural (adsorbing) ligands. Fig. 9 gives an example. Variation of E_i is particularly important in situations where the available instruments do not allow modification of the timing characteristics (see item (2) below). In DPP the possibilities are limited. Amplitude variation and scan reversal would be the counterparts of E_i variation in NPP. However, with the basic nature of DPP being a ramp technique, the possibilities to escape from serious adsorption effects are marginal.

(2) modification of the timing characteristics

As explained in section 2, reduction from an adsorbed layer and diffusion-controlled reduction have different time functionalities (see also Fig. 3). This feature can be utilized by the analyst, both in checking on

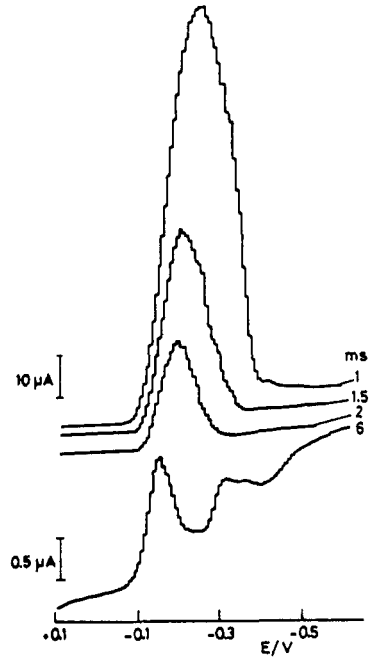

Fig. 8. NPP polarograms of an aqueous $2 \cdot 10^{-4}$ mol·dm^{-3} methylene blue solution. The values of t_p are indicated in ms. Note the immense difference in current scales (from ref. 37).

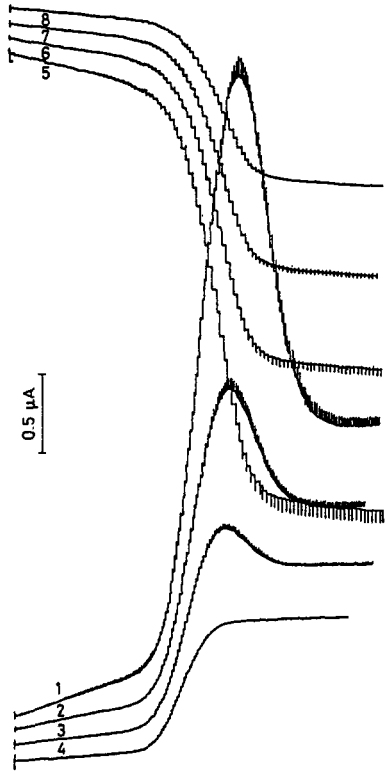

Fig. 9. NPP (1-4) and RPP (5-8) polarograms for a Pb(II)/humic acids solution. E_i = -0,3 V (NPP) and -0.8 V (RPP) vs Ag/AgCl, KCl_{sat}. t_p/ms = 25.3 (1,5), 48.7 (2,6), 84.9 (3,7) and 175 (4,8). (from ref. 38).

the presence of possible adsorption effects, and in getting rid of them. With longer pulse duration, effects of adsorption are always smaller (compare Figs. 8 and 9). The situation is less simple for the duration of the prepulse period, t_0. For small t_0 the amount of adsorbed reactant is relatively low, but the depletion - in terms of reduction of the actual reactant concentration just outside the adsorbed layer - is highest. For a given t_p, the dependence of the NPP limiting current on t_0 may therefore adopt various forms. If the adsorption is strong enough, the curve may even exhibit a minimum. Figure 10 illustrates these features. In avoiding the effects of adsorption one has to choose either a small t_0 (the experiment then is essentially of a d.c. nature) or an extremely large one (which is not very convenient).

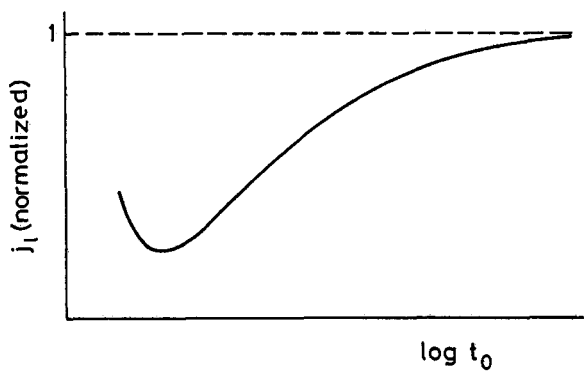

Fig. 10. Schematized dependence of NPP limiting current on prepulse time t_0 for the case of strong linear reactant adsorption. The value of t_p is fixed. The dashed line holds in the absence of adsorption (adapted from [23]).

(3) modification of the measurement mode

In principle it is possible to design modes of pulse polarography in which effects of reactant adsorption are eliminated. The variant recently proposed by Carla et al. [39] constitutes an attempt of this kind. It involves integration of the NPP current from the very beginning of the pulse to a time after the pulse so as to include the potential jump back to E_i. Although the main objective is the elimination of the capacitive current, normalization of the NPP wave is an interesting by-product. The success of the procedure depends on some (rather restrictive) requirements : (i) the adsorption must be so strong that limiting diffusion persists over the whole pre-pulse period, and (ii) the electrochemical conversion of reactant into product should be irreversible.

C. Guidelines for detecting reactant adsorption

To a large extent, the rules for practical observation of reactant adsorption derive from the foregoing treatment. Outer signs of adsorption are most easily found with NPP. For not too weak adsorption, the NPP polarogram bears an outstanding signal in the form of a maximum near the onset of the wave. The argument cannot be used in the opposite sense : absence of a maximum does not prove that adsorption is absent. Other main indicators for the occurrence of reactant adsorption derive from the dependencies of j_ℓ (NPP) and j_p (DPP) on t_p and t_0. As already indicated in section B.2, variation of t_p provides a sensitive tool to inspect adsorption effects. E.g. for NPP, the dependence of j_ℓ on $t_p^{-1/2}$ is affected in a way outlined in Fig. 11. Adsorption results into a decreased slope and a certain intercept. We note that the latter criterion may be somewhat masked by electrode sphericity effects, which also generate a certain (usually relatively small)

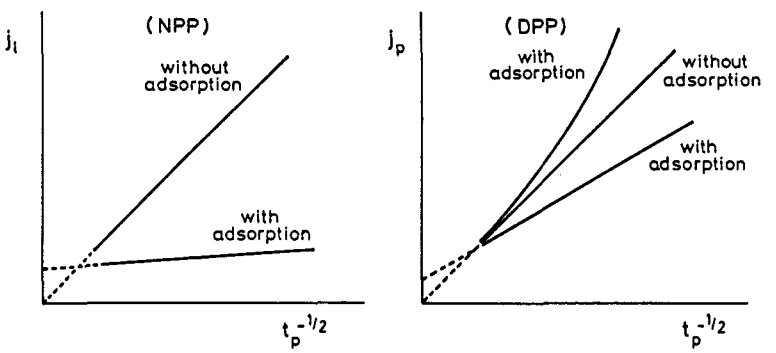

Fig. 11.
Main effect of reactant adsorption on Cottrell plot, ignoring possible deviations caused by electrode sphericity.

intercept. In the limiting case of very strong adsorption and no saturation before the pulse, the Cottrell slope approaches zero and the intercept approaches the value of the d.c. limiting current corresponding to t_0 (tacitly assuming $t_p << t_0$). Variation of t_0 could be used to test this since it amounts to variation of the effective adsorption time. Dependent on the stage of the adsorption at t_0, j_ℓ will either decrease or increase with increasing t_0 (see Fig. 10). Apart from the region around the minimum (which will be only obtained in certain cases of strong adsorption), variation of t_0 provides an excellent practical means to detect adsorption. We add that in the long time limit j_ℓ becomes independent of t_0. This is the regime where adsorption equilibrium is achieved and where the reactant concentration in solution has been fully restored. In this regime - not really important for the usual reactant concentrations and timing characteristics - we find a fully developed current maximum and a normal, *un*depressed limiting current.

Roughly speaking, the above arguments hold for DPP as well as for NPP. However, the situation with DPP incorporates more subtleties. One of them is connected with the extent of reduction of adsorbed reactant. This may be governed not only by the reactant concentration just outside the adsorbed layer, but also by possible potential dependence of the adsorption parameters. Thus, though the variation of j_p with t_p and t_0 may well be less straightforward than for NPP, it still constitutes a powerful means of detecting reactant adsorption in most experimental situations. We finally recall that DPP polarograms only display outer signs of adsorption (such as deformation or splitting of the peak) for cases of relatively strong adsorption.

D. Recommendations for experimental methodology

1. *Potential dependence.* Determine j_{max} and/or j_ℓ as a function of E_i using NPP. Generally the adsorption strength varies with E. The most accurate adsorption data are obtained for potentials where the adsorption is strongest.
2. *Maximum effect of adsorption.* Experiments should preferably be done under conditions such that $j_{max} >> j_d$ (j_d being the diffusion-controlled limiting current density in the absence of adsorption). This is readily observed from the appearance of the voltammogram. If the condition does not hold, decrease c^* or t_p and/or increase t_0.
3. *Linear regime.* Experiments are preferably done in the linear Henry region, unless one wants to study a greater part of the isotherm.
   a. diffusion-controlled transport. Determine j_{max} and/or j_ℓ for various values of c^* and t_0. Plot $j_{max}(j_\ell)$ versus $c^* t_0^{1/2}$. In case of strong adsorption (accumulation by limiting diffusion) all points fall on the same curve. Define the linear range by determining the maximum value of $c^* t_0^{1/2}$ for which $j_{max}(j_\ell)$ versus $c^* t_0^{1/2}$ is linear.
   b. convective transport (long accumulation periods t_0). At fixed convection (constant stirring rate) determine j_{max} and/or j_ℓ as a function of c^* and t_0. Plot $j_{max}(j_\ell)$ versus $c^* t_0$. All points should fall on the same curve. Define the linear regime by determining the maximum $j_{max}(j_\ell)$ for which $j_{max}(j_\ell)$ versus $c^* t_0$ is linear.
4. *Uncompensated resistance.* At a spherical electrode iR-drop increases with electrode radius. Determine $j_{max}(j_\ell)$ at various radii (drop sizes). If j_{max}/A, j_ℓ/A (A being the surface area) increases with A, then iR-drop is confounding the results. To eliminate this problem decrease c^* or t_0, increase t_p, or increase conductivity of the solution.

These factors interact, but are presented in a reasonable order. For example, the dependence of j_{max} on E_i will correctly identify the proper choice of E_i for all following experiments, even if values of t_p are used which introduce uncompensated resistance.

On a static mercury drop electrode (small drop) generally values of t_p are 2-200 ms, those of t_0 0.5-5 s (diffusion) or 1-5 min (convection).

It is perhaps useful to add here that adsorptive accumulation may be successfully combined with pulse stripping techniques such as square-wave voltammetry [40-42]. Methodologically, this is an obvious extension of the analytical utilization of j_{max}, as explained above.

Acknowledgement

The critical comments and suggestions from Prof. Janet G. Osteryoung (Buffalo, U.S.A.) have been helpful in the preparation of this document.

REFERENCES

1. G.J. Patriarche, M. Chateau-Gosselin, J.L. Vandenbalck and P. Zuman in A.J. Bard (Ed.), Electroanalytical Chemistry, Vol. 11, Marcel Dekker, New York, 1979.
2. W.F. Smyth (Ed.), Electroanalysis in Hygiene, Environmental, Clinical and Pharmaceutical Chemistry, Analytical Chemistry Symposia Series, Vol. 2, Elsevier, Amsterdam, 1980.
3. S.A. Borman, Anal. Chem. 54 (1982), 698A (covering R.A. Osteryoung, J.G. Osteryoung and J.J. O'Dea, Pulse Voltammetry - Today and Tomorrow, Pittsburgh Conference, 1982).
4. G.C. Barker and J.A. Bolzan, Z. Anal. Chem. 216 (1966), 215.
5. J.B. Flanagan, K. Takahashi and F.C. Anson, J. Electroanal. Chem. 85 (1977), 257.

6. H.P. van Leeuwen, in ref. 2, p. 383.
7. R. Kalvoda, Anal. Chim. Acta 138 (1982), 11.
8. C.M.G. van den Berg, B.C. Househam and J.P. Riley, J. Electroanal. Chem. 239 (1988), 137.
9. H.P. van Leeuwen, Anal. Chem. 51 (1979), 1322.
10. J. Buffle, A.M. Mota and M.L.S. Simoes Goncalves, J. Electroanal. Chem. 223 (1987), 235.
11. H.P. van Leeuwen, W.F. Threels and R.F.M.J. Cleven, Collect. Czech. Chem. Commun. 46 (1981), 3027.
12. G. Wolff and H.W. Nürnberg, Z. Anal. Chem. 216 (1966), 169.
13. Y. Vaneesorn and W.F. Smyth, in ref. 2, p. 299.
14. E. Palecek, Collect. Czech. Chem. Commun. 39 (1974), 3449.
15. J.J. van der Lee, W.P. van Bennekom and H.J. de Jong, Anal. Chim. Acta 117 (1980), 17.
16. S. Komorsky-Lovrić and M. Lovrić, J. Electroanal. Chem. 190 (1985), 1.
17. M. Lovrić , J. Electroanal. Chem. 197 (1986), 49.
18. A.J. Bard and L.R. Faulkner, Electrochemical Methods, John Wiley & Sons, New York, 1980.
19. J.G. Osteryoung and Schreiner, CRC Critical Riviews in Analytical Chemistry Vol. 19, Suppl. 1 (1988), S1-S27.
20. F.C. Anson, J.B. Flanagan, K. Takahashi and A. Yamada, J. Electroanal. Chem. 67 (1976), 253.
21. J.B. Flanagan, K. Takahashi and F.C. Anson, J. Electroanal. Chem. 81 (1977), 261.
22. H.P. van Leeuwen, J. Electroanal. Chem. 133 (1982), 201.
23. H.P. van Leeuwen, M. Sluyters-Rehbach and K. Holub, J. Electroanal. Chem. 135 (1982), 13.
24. M. Lovrić , J. Electroanal. Chem. 153 (1983), 1
25. K. Holub and H.P. van Leeuwen, J. Electroanal. Chem. 162 (1984), 55.
26. M. Lovrić , J. Electroanal. Chem. 170 (1984), 143.
27. M. Lovrić , J. Electroanal. Chem. 175 (1984), 33.
28. M. Lovrić , J. Electroanal. Chem. 181 (1984), 35.
29. S. Komorsky-Lovrić and M. Lovrić, Electrochim. Acta 30 (1985), 1143.
30. J. Puy, F. Mas, F. Sanz and J. Virgili, J. Electroanal. Chem. 183 (1985), 27; F. Mas, J. Puy, F. Sanz and J. Virgili, J. Electroanal. Chem. 183 (1985), 41, 73; F. Sanz, J. Puy, F. Mas and J. Virgili, J. Electroanal. Chem. 183 (1985), 57.
31. K. Holub and H.P. van Leeuwen, J. Electroanal. Chem. 191 (1985), 281.
32. H.P. van Leeuwen, M. Sluyters-Rehbach and K. Holub, J. Electroanal. Chem. 191 (1985), 293.
33. M. Lovrić, J. Electroanal. Chem. 218 (1987), 77.
34. M. Lovrić, J. Electroanal. Chem. 223 (1987), 271.
35. K. Kobayashi, Chemistry Letters Japan 8 (1988), 1243.
36. J. Galvez and S.-M. Park, J. Electroanal. Chem. 263 (1989), 257, 269; J. Galvez, M.L. Alcaraz and S.-M. Park, J. Electroanal. Chem. 263 (1989), 293.
37. H.P. van Leeuwen, J. Electroanal. Chem. 162 (1984), 67.
38. R.F.M.J. Cleven, Ph.D. Thesis, Wageningen Agricultural University, The Netherlands, 1984.
39. M. Carla, M. Sastre de Vicente, M.R. Moncelli, M.L. Foresti and R. Guidelli, J. Electroanal. Chem. 246 (1988), 283.
40. M. Lovrić, S. Komorsky-Lovrić and R.W. Murray, Electrochim. Acta 33 (1988), 739.
41. M. Lovrić and S. Komorsky-Lovrić, J. Electroanal. Chem. 248 (1988), 239.
42. A. Webber, M. Shah and J.G. Osteryoung, Anal. Chim. Acta 154 (1983), 105; 157 (1984), 1.